A coarse-grained simulation to study the digestion and bioaccessibility of lipophilic nutrients and micronutrients in emulsion

S. Marze

RSC Publishing Food & Function

A coarse-grained simulation to study the digestion and bioaccessibility of lipophilic nutrients and micronutrients in emulsion.

Journal:	*Food & Function*
Manuscript ID:	FO-ART-05-2013-060184.R2
Article Type:	Paper
Date Submitted by the Author:	08-Aug-2013
Complete List of Authors:	Marze, Sebastien; INRA,

Dear Dr Foster,

I acknowledge the decision on my manuscript entitled “A coarse-grained simulation to study the digestion and bioaccessibility of lipophilic nutrients and micronutrients in emulsion”. Following the comments of referee 1 and your recommendation for a minor revision, please find here the new version of the manuscript. All points risen by referee 1 are taken into account except the use of acronyms and the computer code.
The acronyms are kept in order to eliminate long sentences and repetition of words that appear very often in the text. I leave it to the journal editing policy to judge whether the use of abbreviations is appropriate, and if not this will be changed during proof reading. For the computer code, as it will be implemented in the future, our lab does not want to disclose it for the time being. However, the text clearly states the laws that were used, in a quantitative manner, so there is no need to express them as equations. All elements are given so that this work can be replicated using the same software or another one.

I am looking forward to receiving your approval.

Yours sincerely,

Dr. Sébastien Marze
INRA Nantes
Biopolymères, Interactions, Assemblages (BIA)
Interfaces, Systèmes Dispersés (ISD)
Rue de la Géraudière
BP 71627
44316 Nantes cedex 3
Tel : +33 (0)2 40 67 52 38
Fax : +33 (0)2 40 67 50 84
sebastien.marze@nantes.inra.fr

A coarse-grained simulation to study the digestion and bioaccessibility of lipophilic nutrients and micronutrients in emulsion.

Sébastien Marze

UR1268 Biopolymères Interactions Assemblages, INRA, F-44300 Nantes, France

ABSTRACT

The digestion of lipophilic nutrients and micronutrients requires numerous and simultaneous processes of chemical, physical and biological natures. Studying these processes experimentally is challenging, explaining why there is only little information about the mechanisms and interactions involved. Nevertheless, the bioaccessibility of lipophilic micronutrients is poorly understood so new investigation approaches are needed, all the more when digestion of lipophilic nutrients is also involved. In this article, the development of a coarse-grained simulation with no adjustable parameter is reported, enabling the study of the chemical and physical processes controlling bioaccessibility in such systems. The intestinal digestion of a droplet of a pure triglyceride containing a lipophilic vitamin was simulated to obtain their bioaccessibility kinetics (via lipolysis and/or solubilization in bile salt). The parameters examined here were the type of triglyceride, the type of vitamin, the digestive fluid amount, the droplet size, and different digestion conditions reflecting the in vitro or in vivo cases. Among these structure and composition parameters, the type of triglyceride and the digestion conditions had the greatest effects on bioaccessibility. An interplay between triglyceride digestion and micronutrient bioaccessibility kinetics was evidenced, highlighting the roles of the different parameters, in agreement with the experimental literature. This new approach is shown to be relevant to both nutrition and pharmacology.

List of abbreviations

IDF: intestinal digestive fluid, TG: triglyceride, DG: diglyceride, MG: monoglyceride, FA: fatty acid, MN: micronutrient, LR: lipolysis rate, SR: solubilization ratio, CTS: computation time step, MCT: medium chain triglyceride, LCT: long chain triglyceride, TC: tricaprylin, TO: triolein, TEP-DH: trieicosapentaenoin and tridocosahexaenoin, EPA: eicosapentaenoic acid, DHA: docosahexaenoic acid, vitA: vitamin A, vitE: vitamin E.

1. Introduction

Because the digestion of nutrients and micronutrients consists of complex interdependent processes, its parameters and mechanisms are not well known, all the more since they are of several natures, essentially chemical, physical and biological. The study of the whole digestion of a (micro)nutrient requires these three sciences, as the endpoint is generally the bioavailability, that is the proportion used by the tissues as delivered by the systemic circulation.[1] In practice, there are so many processes from the ingestion to the use that only biological aspects are classically studied. However, the chemical and physical processes in the digestive tube constitute the first step, shown to be critical for many food structures and formulations.[2,3] The endpoint of this first step is called bioaccessibility and is the proportion of a (micro)nutrient transformed in its absorbable form. This is equivalent to the proportion of drug released in pharmacology. In both domains, the molecule has to be liberated from its matrix and prepared for absorption. To do so, chemical processes such as hydrolysis and physical aspects such as structures evolution and molecular diffusion act simultaneously. So such processes have to be studied simultaneously in order to identify their parameters and interactions. This is experimentally challenging to achieve, and requires a simplification to model foods, such as emulsions. Such model foods may also be simulated, giving the opportunity to understand the mechanisms involved for their digestion. Generic simulations

exist mostly for bioavailability of drugs[4-10] or hydrolysis of nutrients[11-14] and only few establish a kinetic relation between one of these aspects and the matrix structural parameters.[15,16] Promising methods enabling simulation of such dynamic complex systems consist of working at a coarse-grained scale, where the fine molecular structure is not taken into account, the smallest element being either a functional group of the molecule, the molecule itself, or an assembly of molecules. This allows an expansion of the simulated space and time scales, making the link between microscopic and mesoscopic levels possible.[17]

In this article, a model is build to study by coarse-grained simulation the role of the parameters influencing the bioaccessibility kinetics of lipophilic nutrients and micronutrients in emulsion during intestinal digestion. The effect of each parameter is studied independently, with an emphasis in the interactions between lipophilic nutrients and micronutrients, poorly known in the literature. All processes, including the main ones, lipolysis and solubilization in bile salt, are simulated from molecular knowledge, using no adjustable parameter. The results are interpreted in order to reveal the interplay between lipolysis and solubilization of glycerides and solubilization of micronutrients.

2. Simulation methods

NetLogo 4.1.3 was used to build the simulation. It is an agent-based modeling software using the Logo programming language. It is able to operate multiple agents independently and works in both 2D and 3D.[18]

2.a. Geometry

The model simulates a single lipid droplet stabilized by an interfacial layer and dispersed in an intestinal digestive fluid (IDF). It is built in 2 dimensions (2D). A square is used to represent the droplet in order to simplify the control of the interfacial layer particles during the digestion. This does not affect the specific interfacial length as the perimeter to surface

area ratio is the same for a square and a circle. A square simulation box is defined, with a length of 316 patches and periodic boundary conditions. The droplet is set so that its equivalent volume ranges from 0.4 to 3% of the total simulation box equivalent volume, thus representing a dilute emulsion. The droplet length *d* ranges from 100 to 50 patches. The dimensions were chosen in order to limit the total number of particles in the simulation. The initial number of triglycerides (TG) is set to $(d-1)^2/3$, so that the number of final digestion products, that are fatty acids (FA) and monoglycerides (MG), (FA+MG = 3.TG) equals the initial number of patches inside the droplet. The initial number of lipophilic micronutrient (MN) is set to 0.2% of the number of FA+MG. The density of the droplet is assumed to remain constant during digestion.

2.b. Particles

Each type of molecule is defined as an agent, drawn as a specific round particle. For each type of molecule, a single particle represents a mass unity. Each simulation box patch can only be occupied by one particle at a time. Initially, TG and MN particles are set at random positions inside the droplet (lipid phase) whereas IDF particles are set at random positions outside the droplet (aqueous phase). The bile salt and lipase are not distinguished in this simulation so each IDF particle is actually defined as a bile/lipase complex, which was demonstrated to be the active form at the oil/water interface of emulsion.[19] The concentration is such that lipase is in excess and bile salt is above its critical micelle concentration, so each IDF particle is actually a micelle. The interfacial layer is represented by particles situated on the patches delimiting the droplet perimeter. Using a random walk scheme, each particle is free to diffuse in its environment delimited by the interfacial layer particles, the latter being immobile. The step lengths of the walk for the lipid particles are set relatively to each others as a ratio between the square root of their diffusion coefficients determined from the Stokes-Einstein equation according to the molar mass and the local viscosity.[20] The MN are assumed to have

the same solubility in each glyceride class (some literature reports an increased solubility in the digestion products[21-24]), so the step length of their walk is set for an averaged lipid phase viscosity, according to their molar mass. At each computation time step, the IDF particles are displaced to random positions outside the droplet, reflecting the much higher diffusion coefficient for these particles compared to the lipid ones, and also the possible convection of the whole droplet relative to the aqueous phase.

2.c. Digestion

The simulated digestion consists of lipolysis with specific lipolysis rates (LR) and solubilization of the digestion products and MN in the digestive micelles with specific solubilization ratios (SR, mass of solubilizate/mass of bile salt). Table 1 reports some literature experimental values for LR and SR. The lipolysis reactions 1TG $\rightarrow$ 1DG + 1FA and 1DG $\rightarrow$ 1MG + 1FA where DG are the diglycerides, are used to generate the digestion products, eventually resulting in a MG:FA molecular ratio of 1:2. The difference due to the mass basis of the calculations was neglected as it is small but would imply different fractional reactions depending on the TG used. In practice, the interfacial layer particles are initially set to green. During the simulation, each time a IDF particle is on a patch in contact with an interfacial layer particle, the latter becomes red to signify a IDF particle adsorption. A reaction occurs when a TG or a DG particle is in contact with a red interfacial layer particle, the latter becoming green again to signify IDF particle inactivation. Depending on the lipolysis rate, which is assumed to be the same for TG and DG,[38] the reaction is complete after a given number of contacts, inversely proportional to the LR. Similarly, partial solubilization occurs when a MG, a FA or a MN particle is in contact with a red interfacial layer particle, the latter becoming green again to signify bile solubilization. Depending on the solubilization ratio, the complete solubilization occurs after a given number of contacts, inversely proportional to the SR. In a simulation reflecting in vitro conditions where digestive

micelles are assumed to saturate with solubilizates, the number of IDF particles is decreased in proportion to the number of contacts needed to solubilize the digestion products and MN. In a simulation reflecting in vivo conditions where digestive micelles are assumed to empty during lipid absorption and recycle for other solubilizates,[39,40] the number of IDF particles is set constant. In all cases, lipolysis reactions do not reduce the number of IDF particles. To conserve the density, the perimeter of the droplet is decreased as particles leave the lipid phase. All particles are counted at each computation time step and the result is expressed either as relative proportions of different particles or as a bioaccessibility. The latter is expressed for FA, MG and MN as the proportion of particles solubilized in bile salt relative to the amount of particles initially inside the droplet (2.TG for FA and 1.TG for MG). The digestion products are counted once they are solubilized in bile salt, not when they are still inside the droplet after lipolysis. The kinetics of bioaccessibility is characterized by the half life, that is the time (given as the number of computation time steps, CTS) at which half of the final bioaccessibility is reached. This enables a direct comparison of the effect of each parameter that does not require the fitting with a specific model. In summary, fig. 1 presents a diagram illustrating the model used for the simulation.

2.d. Systems under study

The systems were chosen on the basis of the availability of digestion data in the literature, where mostly MCT oils (usually composed of caprylic and capric acids) and LCT vegetable oils (usually rich in oleic and linoleic acids) are represented. Thus, the digestion of tricaprylin (TC) and triolein (TO) were investigated, as well as a model long chain n-3 triglyceride interpolated from trieicosapentaenoin and tridocosahexaenoin (TEP-DH). To model integer data, the LR values of table 1 were rounded to 2, 1 and 1/6 respectively, and the SR values for digestion products (considering that FA and MG have the same SR) were rounded to 3.5, 0.5 and 0.1 respectively. The latter was extrapolated by noticing that ln(SR) as a function of the

number of carbons in the aliphatic chain n follows a linear law of the form ($-0.5.n + b$) for saturated MG and FA. For unsaturated glycerides, data are available only for oleic acid, monoolein and linoleic acid, with a common SR value around 0.5. An extrapolation from this value to n=21 using a linear law with the same slope gives a SR of approximately 0.1 for TEP-DH digestion products. The SR of lipophilic MN is not well documented, in contrast with lipophilic drugs.[41] Nethertheless, some SR were measured for a few vitamins and sterols. Vitamins A and E (retinol abbr. vitA and α-tocopherol abbr. vitE) were chosen because they present a low and a high SR respectively. Again, the SR values were rounded, to 0.005 and 0.1 respectively. The initial number of IDF particles was set as a ratio of the expected number of particles of digestion products (3.TG), of 0.5, 1 or 2, which is in the typical range for the bile salt/(FA+MG) ratio evaluated from in vivo studies.[42-44]

In summary, the parameters that were varied in the present simulation were the IDF particles conditions (saturated or recycled, IDF/(FA+MG) ratio), the types of triglyceride and of micronutrient, and the size of the droplet (square of length of 50, 75 or 100). The number of particles treated simultaneously during the simulation ranged typically between 10000 and 30000. Several simulations could be run simultaneously on a dedicated normal PC, with a duration ranging typically between 0.5 and 5 h.

All simulations were run in triplicate and the results are given as averages and standard deviations.

3. Results

First, control simulations with no MN were run to define the contact rules needed to reproduce the relative LR between the three TG in various conditions. In these simulations, only lipolysis was taken into account and no solubilization was permitted, therefore the droplet size and the number of IDF particles remained constant. When the relative LR were

recovered, simulations with solubilization and no MN were run to quantify the contribution of the solubilization of the lipolysis products in the same conditions. For TC, the half life was not affected within 10% whereas for TO and TEP-DH, it was increased by a factor 2.3 ± 0.3 and 1.7 ± 0.1 respectively. This shows that the limiting process is lipolysis for TC and solubilization for TO and TEP-DH.

Then, full simulations with MN were run. Tables 2-5 report the final bioaccessibility and half life of FA and MN for all conditions described in the methods part. First, FA final bioaccessibility and FA half life do not significantly differ depending on the MN, and are also similar for the simulations with no MN (results not shown). Then, FA final bioaccessibility ranges from 4.5% to 100% and FA half life may differ by a factor of more than 60 depending on the conditions, the greatest effect being due to the TG chain length. Similarly, MN final bioaccessibility ranges from 2.5% to 100% and MN half life may differ by a factor of more than 60 depending on the conditions, the greatest effect being due to the bile condition (saturated or recycled). These results will be commented in the discussion part.

Here, a few representative results are presented starting in fig. 2 with pictures from a simulation in a case where bile is saturated. The different types of particles are visible, from pure TG/MN to mixed TG/DG/MG/FA/MN inside the droplet. Obviously, the number of IDF particles decreases. Note that the digestion products are mainly located near the interface before solubilization (after, they are removed from the simulation together with the IDF particles). The relative percentages of each glyceride are given in fig. 3 in another case where bile is saturated, showing an incomplete digestion due to a limiting number of bile salt. These relative percentages should not be confused with bioaccessibility, the maximum for the digestion products being 66.7 % for FA and 33.3% for MG. For the same conditions, those values are indeed reached in the case where bile is recycled, providing bile salt in excess

hence a complete digestion (fig. 4). Note that all glycerides except DG display sublinear kinetics.

Fig. 5 shows the main results allowing a comparison between the digestion of the three TG+vitA systems in a case where bile is saturated. Very different kinetics are obtained, only TC being completely digested, as illustrated by the 100% bioaccessibility of its fatty acids. This is reflected in the decrease of the droplet length which is complete for TC, only partial for TO and very limited for TEP-DH. In contrast, the vitA bioaccessibility is low in all systems, although the same ordering is recovered. Note that all kinetics are sublinear except for vitA in TC being superlinear.

In fig. 6, the same systems are compared in a case where bile is recycled. Again the kinetics are very different depending on the system, but here all TG digestions are complete. The ordering for all quantities is the same as in fig. 5, but here all vitA kinetics are superlinear and higher values are reached for TO and TEP-DH.

Note that all sublinear bioaccessibility curves actually display the typical shape associated to lipid digestion kinetics. In contrast, the shape of the superlinear bioaccessibility curves was unexpected.

4. Discussion

In this part, the results in the tables are described in terms of trends which are compared to experimental data from the literature. All the trends are statistically significant except when mentioned. Then, the simulation is discussed in the context of available models and simulations of the literature.

4.a. Effect of the triglyceride

Except when bile is recycled where final FA bioaccessibility is always 100%, tables show that final FA bioaccessibility decreases and FA half life increases with the chain length of TG.

This is an expected result due to both LR and SR decreasing as a function of the chain length of TG (see table 1 and ref. 3).

When bile is saturated, final MN bioaccessibility decreases with the chain length of TG and MN half life is not significantly affected. When bile is recycled, final MN bioaccessibility increases and MN half life increases with the chain length of TG. This contradiction is reflected in the literature. Most authors reported an increase of MN bioaccessibility with the chain length of TG in vitro[45-53] and in vivo.[54-61] Nevertheless, some authors reported a decrease of MN bioaccessibility with the chain length of TG (refs. 52-53 for fish oil, and refs. 62-66) or no clear effect of the chain length of TG (ref. 46 for lutein, and refs. 23,24,67,68).

The present simulation when bile is recycled shows that increasing the chain length of TG results in longer digestion, giving more time for MN to solubilize in bile salt, hence a higher MN bioaccessibility. Thus, an interplay is evidenced between the duration of the TG digestion and the MN bioaccessibility. In fact, the same would be true if bile was in excess in the cases where bile is saturated, as proven by fig. 7 showing that MN bioaccessibility as a function of FA bioaccessibility is almost not affected by the bile condition. Fig. 7 also suggests that the relation between these bioaccessibilities is not strictly linear as postulated by several authors,[69-70] but might rather be superlinear with seemingly linear parts. This superlinearity could be due to the evolution of the droplet length, decreasing towards the molecular diffusion length as digestion progresses.

4.b. Effect of the micronutrient

Whatever the other conditions are, vitE always shows a higher final MN bioaccessibility and shorter MN half life than vitA. No data are available to check this prediction and the in vivo data of absorption are highly variable, typically from 50 to 90%,[71] making a direct comparison difficult.

The type of MN does not significantly affect final FA bioaccessibility and FA half life, which is an expected result as the concentration of MN in TG is very low.

4.c. Effect of the IDF/(FA+MG) ratio

When bile is saturated, final bioaccessibility increases and half life increases with the IDF/(FA+MG) ratio, except for TC where final bioaccessibility is not significantly affected and half life decreases with the IDF/(FA+MG) ratio, showing that bioaccessibility is more efficient at high IDF/(FA+MG) ratios. For TEP-DH, even though the mean half life increases with the IDF/(FA+MG) ratio, the difference is not always significant taking the standard deviation into account. For TO+vitE, the trend of the MN half life is uncertain.

When bile is recycled, whatever the other conditions are, final bioaccessibility is not significantly affected and half life decreases with the IDF/(FA+MG) ratio.

The literature shows that when the concentration of IDF increases at constant glycerides concentration (as in the present simulation), the lipolysis and bioaccessibility of glycerides[72-75] and the bioaccessibility of lipophilic MN[75-78] follow non-monotonic curves with a maximum plateau at intermediate concentrations. Reciprocally, when the concentration of glycerides increase at constant IDF concentration, the same non-monotonic trends are reported for lipolysis and bioaccessibility of glycerides[48,50,73,74] and the bioaccessibility of lipophilic MN.[46,48,50,52,59,61,79]

The present simulation recovers these results, what may again be understood as an interplay between the duration of the TG digestion and the MN bioaccessibility. When bile is saturated (equivalent to high TG or low IDF concentrations), the digestion duration decreases with decreasing IDF/(FA+MG) ratio (increasing TG concentration), giving less time for the MN to solubilize hence a lower MN bioaccessibility. When bile is recycled (equivalent to intermediate TG or IDF concentrations), the digestion duration increases with decreasing IDF/(FA+MG) ratio (increasing TG concentration), giving more time for the MN to

solubilize, but resulting in a MN bioaccessibility plateau because the duration of the MN solubilization also increases.

4.d. Effect of the droplet size

Whatever the other conditions are, final FA bioaccessibility is not significantly affected and FA half life decreases with the droplet length. This is a known effect of the specific interfacial area (increasing with the droplet length in this single droplet simulation), of which the increase results in faster glycerides digestion and bioaccessibility (see refs. in [3]). This should not be confused with the effect of the droplet size in emulsion where the number of droplets and the dispersed volume fraction may also vary, making the specific interfacial area and the droplet size inversely proportional.[20]

For the vitA systems, final MN bioaccessibility increases with the droplet length and MN half life is not significantly affected, except for TC where MN half life decreases with the droplet length. For TC+vitA when bile is recycled, the trend of the final MN bioaccessibility is uncertain. For the vitE systems, final MN bioaccessibility and MN half life are not significantly affected by the droplet length. The same effect of the specific interfacial area explains these results, but vitE is less affected because it is always solubilized faster and to a higher extent. In the literature, recent articles reported an increasing MN bioaccessibility with decreasing particle size,[78,80-83] or increasing specific interfacial area, thus in agreement with the present simulation results.

4.e. Effect of the bile condition

When bile is recycled, final FA bioaccessibility is always 100% because this is the endpoint of the simulation. So it is always equal or higher than when bile is saturated. At a comparable final FA bioaccessibility of 100% (for TC systems), FA half life is not significantly affected by the bile condition.

Final MN bioaccessibility and MN half life are always greater when bile is recycled than when bile is saturated, except for TC systems where the differences are not statistically significant.

These results may explain the high variability of bioaccessibility and bioavailability data found in the literature,[3,71] especially when in vitro and in vivo data are compared. The absorption of EPA and DHA was indeed found to be higher than 98% in vivo,[84] whereas the bioaccessibility was about 50% in a static in vitro study.[85] The present simulation shows that in most static in vitro cases, bile salt is in lower total concentration than in vivo, limiting glycerides and lipophilic MN solubilization. However, fig. 7 suggests that in excess presence of bile salt, the in vitro cases would follow the same MN bioaccessibility vs. FA bioaccessibility curve as the in vivo cases. Nevertheless, it is known that a high bile salt concentration inhibits lipolysis,[72,74] so using dynamic in vitro methods is preferable.[86]

4.f. Comparison to other simulations

With a similar aim in mind, that is studying digestion and/or bioavailability, hydrolysis modeling by enzymologists[11-14] or generic dissolution/absorption simulations by pharmacologists[4-10] treated one part of the present problem, and did not consider the detailed matrix structural parameters (only a size is included in the dissolution number by pharmacologists). When hydrolysis and solubilization both affect the structure, only a few attempts exist in the literature by food scientists.[15,16,87] Nevertheless, none of these are completely satisfactory, because these do not include MN and either treat hydrolysis and solubilization with a single parameter,[15,16] or neglect the matrix structural details.[87] Moreover, all communities use adjustable parameters, which are not always linked to experimentally measurable quantities.

The present bioaccessibility simulation is able to take all these aspects into account (not including absorption) with no adjustable parameter, the required molecular properties coming

from experimentally measurable quantities of the literature. It recovers the typical lipolysis profiles modeled by enzymologists[11-14] (fig. 3). It confirms the roles of the formulation and structural parameters at different scales from microscopic (interface) to mesoscopic (droplet size) found for TG digestion,[15,16] and extends those to lipophilic MN bioaccessibility. It thus precises the parameters that could be used by pharmacologists to specifically design emulsion-based drug dosage formulations.

5. Conclusion

To highlight the results, first the coarse-grained simulation presented here is only based on experimentally measurable quantities, using no adjustable parameter. Then, although it is a single droplet model, it features the same parameters than for emulsion, and enables the study of their effects independently. Applied to lipophilic (micro)nutrients digestion and bioaccessibility, it was able to identify the limiting processes as well as the mechanisms responsible for the effects of each parameter. This new approach is thus promising to formulate emulsion-based foods or drugs. The present simulation constitutes a fundamental starting point, but is flexible so independent particles could be used for bile and lipase, or the role of calcium on the formation of salts of saturated fatty acids could be integrated, for instance. It will be refined to gain realism by using e.g. triglycerides mixtures, different emulsifiers and their competition or inhibition at interface, a gastric step, multiple nutrients and associated hydrolases (mainly proteases), other lipophilic micronutrients, mixed micelles structure, micronutrient solubility in digestion products. Another improvement will be to make the time step explicit in order to be fully quantitative. To validate the effects of these parameters, a dynamic experimental setup is currently designed to reproduce the conditions of a single droplet digestion, and overcome the limitations of static in vitro methods.

Acknowledgments

The author acknowledges the ISC-PIF (Paris Île-de-France Complex Systems Institute) for the IDEAS workshop (Ideas for Design, knowledge Engineering Applied to living complex Systems), Olivier Vitrac (INRA Île-de-France) for his introduction to coarse-grained simulation, and the Carnot Institute Qualiment for financial support.

References

1 S. J. Fairweather-Tait and S. Southon, in Encyclopedia of Food Sciences and Nutrition, ed. B. Caballero, L. Trugo and P. Finglas, Academic Press, London, 2003, pp. 478-484.

2 J. Parada and J. M. Aguilera, *J. Food Sci.*, 2007, **72**, R21-R32.

3 S. Marze, *Crit. Rev. Food Sci. Nutr.*, 2013, **53**, 76-108.

4 G. L. Amidon, H. Lennernäs, V. P. Shah and J. R. Crison, *Pharm. Res.*, 1995, **12**, 413-420.

5 L. X. Yu, E. Lipka, J. R. Crison and G. L. Amidon, *Adv. Drug Deliver. Rev.*, 1996, **19**, 359-376.

6 M. N. Martinez and G. L. Amidon, *J. Clin. Pharmacol.*, 2002, **42**, 620-643.

7 K. S. Pang, *Drug Metab. Dispos.*, 2003, **31**, 1507-1519.

8 S. Willmann, W. Schmitt, J. Keldenich, J. Lippert and J. B. Dressman, *Med. Chem.*, 2004, **47**, 4022-4031.

9 K. Sugano, *Chem. Biodivers.*, 2009, **6**, 2014-2029.

10 K. Sugano, *Int. J. Pharm.*, 2010, **398**, 73-82.

11 C. S. Wang, J. A. Hartsuck and D. Downs, *Biochemistry*, 1988, **27**, 4834-4840.

12 H. Hermansyah, M. Kubo, N. Shibasaki-Kitakawa and T. Yonemoto, *Biochem. Eng. J.*, 2006, **31**, 125-132.

13 H. Hermansyah, A. Wijanarko, M. Kubo, N. Shibasaki-Kitakawa and T. Yonemoto, *Bioprocess. Biosyst. Eng.*, 2010, **33**, 787-796.

14 D. A. Mitchell, J. A. Rodriguez, F. Carrière, J Baratti and N. Krieger, *J. Biotechnol.*, 2008, **133**, 343-350.

15 Y. Li and D. J. McClements, *J. Agric. Food Chem.*, 2010, **58**, 8085-8092.

16 S. Marze and M. Choimet, *Soft Matter*, 2012, **8**, 10982-10993.

17 A. N. Gorban, N. K. Kazantzis, I. G. Kevrekidis, H. C. Öttinger and C. Theodoropoulos (Eds.), Model Reduction and Coarse-Graining Approaches for Multiscale Phenomena, Springer Berlin Heidelberg, New York, 2006.

18 U. Wilensky, 1999. NetLogo. http://ccl.northwestern.edu/netlogo/. Center for Connected Learning and Computer-Based Modeling, Northwestern University, Evanston, IL.

19 D. Lairon, G. Nalbone, H. Lafont, J. Leonardi, J. L. Vigne, C. Chabert, J. C. Hauton and R. Verger, *Biochim. Biophys. Acta*, 1980, **618**, 119-128.

20 S. Marze, M. Choimet and L. Foucat, *Soft Matter*, 2012, **8**, 10994–11004.

21 D. J. W. Grant and I. K. A. Abougela, *Int. J. Pharm.*, 1983, **17**, 77-89.

22 S. Meguro, K. Higashi, T. Hase, Y. Honda, A. Otsuka, I. Tokimitsu and H. Itakura, *Eur. J. Clin. Nutr.*, 2001, **55**, 513-517.

23 G. A. Kossena, B. J. Boyd, C. J. H. Porter and W. N. Charman, *J. Pharm. Sci.*, 2003, **92**, 634-648.

24 G. A. Kossena, W. N. Charman, B. J. Boyd, D. E. Dunstan and C. J. H. Porter, *J. Pharm. Sci.*, 2004, **93**, 332-348.

25 B. Entressangles, L. Paséro, P. Savary, L. Sarda and P. Desnuelle, *Bull. Soc. Chim. Biol.*, 1961, **43**, 581-591.

26 R. G. Jensen, J. Sampugna, R. M. Parry Jr., K. M. Shahani and R. C. Chandan, *J. Dairy Sci.*, 1962, **45**, 1527-1529.

27 B. M. Laws and J. H. Moore, *Biochem. J.*, 1963, **87**, 632-638.

28 Y. K. Yip, S. Ramachandran and S. R. Wagle, *P. Soc. Exp. Biol. Med.*, 1975, **149**, 683-687.

29 C. S. Wang, A. Kuksis and F. Manganaro, *Lipids*, 1982, **17**, 278-284.

30 L. Y. Yang, A. Kuksis and J. J. Myher, *J. Lipid Res.*, 1990, **31**, 137-147.

31 I. Ikeda, E. Sasaki, H. Yasunami, S. Nomiyama, M. Nakayama, M. Sugano, K. Imaizumi and K. Yazawa, *Biochim. Biophys. Acta*, 1995, **1259**, 297-304.

32 Y. Yang and M. E. Lowe, *J. Lipid Res.*, 2000, **41**, 48-57.

33 A. F. Hofmann, *Biochim. Biophys. Acta*, 1963, **70**, 306-316.

34 C. P. Freeman, *Br. J. Nutr.*, 1969, **23**, 249-263.

35 M. El-Gorab and B. A. Underwood, *Biochim. Biophys. Acta*, 1973, **306**, 58-66.

36 J. Imai, M. Hayashi, S. Awazu and M. Hanano, *Chem. Pharm. Bull.*, 1983, **31**, 4077-4082.

37 P. B. Nielsen, A. Müllertz, T. Norling and H. G. Kristensen, *Int. J. Pharm.*, 2001, 222, 217-224.

38 J. A. Rodriguez, Y. Ben Ali, S. Abdelkafi, L. D. Mendoza, J. Leclaire, F. Fotiadu, G. Buono, F. Carrière and A. Abousalham, *Biochim. Biophys. Acta*, 2010, **1801**, 77-83.

39 J. M. Dietschy, *J. Lipid Res.*, 1968, **9**, 297-309.

40 C. T. Phan and P. Tso, *Front. Biosci.*, 2001, **6**, 299-319.

41 T. S. Wiedmann and L. Kamel, *J. Pharm. Sci.*, 2002, **91**, 1743-1764.

42 B. Borgström, A. Dahlqvist, G. Lundh and J. Sjövall, *J. Clin. Invest.*, 1957, **36**, 1521-1536.

43 M. Rautureau and J. C. Rambaud, *Gut*, 1981, **22**, 393-397.

44 P. L. Zentler-Munro, D. R. Fine, W. J. F. Fitzpatrick and T. C. Northfield, *Gut*, 1984, **25**, 491-499.

45 A. von Bonsdorff-Nikander, L. Christiansen, L. Huikko, A. M. Lampi, V. Piironen, J. Yliruusi and A. M. Kaukonen, *Lipids*, 2005, **40**, 181-190.

46 T. Huo, M. G. Ferruzzi, S. J. Schwartz and M. L. Failla, *J. Agric. Food Chem.*, 2007, **55**, 8950-8957.

47 B. Nidhi and V. Baskaran, *J. Am. Oil Chem. Soc.*, 2011, **88**, 367-372.

48 K. Ahmed, Y. Li, D. J. McClements and H. Xiao, *Food Chem.*, 2012, **132**, 799-807.

49 C. Qian, E. A. Decker, H. Xiao and D. J. McClements, *Food Chem.*, 2012, **135**, 1440-1447.

50 L. Salvia-Trujillo, C. Qian, O. Martín-Belloso and D. J. McClements, *Food Chem.*, 2013, **139**, 878-884.

51 Y. Yang and D. J. McClements, *Food Chem.*, 2013, doi: http://dx.doi.org/10.1016/j.foodchem.2013.03.033.

52 I. J. P. Colle, S. van Buggenhout, L. Lemmens, A. M. van Loey and M. E. Hendrickx, *Food Res. Int.*, 2012, **45**, 250-255.

53 I. J. P. Colle, L. Lemmens, S. van Buggenhout, K. Met, A. M. van Loey and M. E. Hendrickx, *Food Res. Int.*, 2013, **51**, 32-38.

54 C. Sylvén and B. Borgström, *J. Lipid Res.*, 1969, **10**, 351-355.

55 I. Holmberg, L. Aksnes, T. Berlin, B. Lindbäck, J. Zemgals and B. Lindeke, *Biopharm. Drug Dispos.*, 1990, **11**, 807-815.

56 D. Behrens, R. Fricker, A. Bodoky, J. Drewe, F. Harder and M. Heberer, *J. Pharm. Sci.*, 1996, **85**, 666-668.

57 P. Borel, V. Tyssandier, N. Mekki, P. Grolier, Y. Rochette, M. C. Alexandre-Gouabau, D. Lairon and V. Azaïs-Braesco, *J. Nutr.*, 1998, **128**, 1361-1367.

58 S. M. Caliph, W. N. Charman, C. J. H. Porter, *J. Pharm. Sci.*, 2000, **89**, 1073-1084.

59 C. J. H. Porter, A. M. Kaukonen, A. Taillardat-Bertschinger, B. J. Boyd, J. M. O'Connor, G. A. Edwards and W. N. Charman, *J. Pharm. Sci.*, 2004, **93**, 1110-1121.

60 C. J. H. Porter, A. M. Kaukonen, B. J. Boyd, G. A. Edwards and W. N. Charman, *Pharm. Res.*, 2004, **21**, 1405-1412.

61 K. W. Y. Lee, C. J. H. Porter and B. J. Boyd, *J. Pharm. Sci.*, 2013, **102**, 565-578.

62 A. M. Kaukonen, B. J. Boyd, C. J. H. Porter and W. N. Charman, *Pharm. Res.*, 2004, **21**, 245-253.

63 A. M. Kaukonen, B. J. Boyd, W. N. Charman and C. J. H. Porter, *Pharm. Res.*, 2004, **21**, 254-260.

64 A. Dahan and A. Hoffman, *Pharm. Res.*, 2006, **23**, 2165-2174.

65 A. Dahan and A. Hoffman, *Eur. J. Pharm. Biopharm.*, 2007, **67**, 96-105.

66 H. Yu, K. Shi, D. Liu and Q. Huang, *Food Chem.*, 2012, **131**, 48-54.

67 G. A. Kossena, W. N. Charman, B. J. Boyd and C. J. H. Porter, *J. Pharm. Sci.*, 2005, **94**, 481-492.

68 M. Grove, G. P. Pedersen, J. L. Nielsen and A. Müllertz, *J. Pharm. Sci.*, 2005, **94**, 1830-1838.

69 P. Borel, P. Grolier, M. Armand, A. Partier, H. Lafont, D. Lairon and V. Azais-Braesco, *J. Lipid Res.*, 1996, **37**, 250-261.

70 A. Malaki-Nik, M. Corredig and A. J. Wright, *Mol. Nutr. Food Res.*, 2011, **55**, S278-S289.

71 G. F. M. Ball, Vitamins in foods: analysis, bioavailability, and stability, CRC Press, Boca Raton, FL, 2006.

72 B. Borgström and C. Erlanson, *Eur. J. Biochem.*, 1973, **37**, 60-68.

73 F. J. Alvarez and V. J. Stella, *Pharm. Res.*, 1989, **6**, 449-457.

74 Y. Li, M. Hu and D. J. McClements, *Food Chem.*, 2011, **126**, 498-505.

75 R. Devraj, H. D. Williams, D. B. Warren, A. Müllertz, C. J. H. Porter and C. W. Pouton, *Int. J. Pharm.*, 2013, 441, 323-333.

76 G. T. Rich, R. M. Faulks, M. S. J. Wickham and A. Fillery-Travis, *Lipids*, 2003, **38**, 947-956.

77 A. J. Wright, C. Pietrangelo and A. MacNaughton, *Food Chem.*, 2008, **107**, 1253-1260.

78 P. Wang, H. J. Liu, X. Y. Mei, M. Nakajima and L. J. Yin, *Food Hydrocolloids*, 2012, **26**, 427-433.

79 T. Sanz and H. Luyten, *Food Hydrocolloids*, 2007, **21**, 203-211.

80 E. Acosta, *Curr. Opin. Colloid Interface Sci.*, 2009, **14**, 3-15.

81 M. M. R. M. M. Affandi, T. Julianto and A. B. A. Majeed, *Food Sci. Technol. Res.*, 2012, **18**, 549-554.

82 K. R. N. Moelants, L. Lemmens, M. Vandebroeck, S. van Buggenhout, A. M. van Loey and M. E. Hendrickx, *J. Agric. Food Chem.*, 2012, **60**, 11995-12003.

83 L. Salvia-Trujillo, C. Qian, O. Martín-Belloso and D. J. McClements, *Food Chem.*, 2013, doi: http://dx.doi.org/10.1016/j.foodchem.2013.03.050.

84 L. Sanguansri, Z. Shen, R. Weerakkody, M. Barnes, T. Lockett and M. A. Augustin, *Food & Function*, 2013, **4**, 74-82.

85 S. Marze, A. Meynier and M. Anton, *Food & Function*, 2013, **4**, 231-239.

86 A. Guerra, L. Etienne-Mesmin, V. Livrelli, S. Denis, S. Blanquet-Diot and M. Alric, *Trends Biotechnol.*, 2012, **30**, 591-600.

87 M. Taghipoor, P. Lescoat, J. R. Licois, C. Georgelin and G. Barles, *J. Theor. Biol.*, 2012, **294**, 114-121.

Molecules	n	LR	SR (FA)	SR (MG)
Caprylic glycerides	8	2.06 ± 0.97		3.5
Capric glycerides	10	1.56 ± 0.62		0.88
Lauric glycerides	12	1.06 ± 0.34	0.78	0.58
Myristic glycerides	14	0.596 ± 0.336		0.16
Palmitic glycerides	16	0.362 ± 0.245	0.086	0.053
Stearic glycerides	18	0.283 ± 0.283	0.042	
Oleic glycerides	18*	1	0.62	0.52
Linoleic glycerides	18*		0.48	
Eicosapentaenoic glycerides	20*	0.162 ± 0.027		
Docosahexaenoic glycerides	22*	0.158 ± 0.071		
Retinol (vitA)				0.0043
α-tocopherol (vitE)				0.12 ± 0.06

Table 1: Data from the literature for the lipolysis rate of triglycerides normalized to triolein (LR), and the mass by mass solubilization ratio (SR) for fatty acids FA or monoglycerides MG in bile salts. LR are given as averages and standard deviations from the values in refs. 25-32. SR for monoglycerides are from Hofmann.[33] SR for fatty acids are from Freeman.[34] SR for retinol is from El-Gorab.[35] SR for α-tocopherol is given as an average and standard deviation from the values in refs. 36-37. The stars identify the unsaturated glycerides.

IDF/(FA+MG) mass ratio	TC+vitA	TO+vitA	TEP-DH+vitA	TC+vitE	TO+vitE	TEP-DH+vitE
Bile is saturated						
0.5	100.0 ± 0.0 144 ± 7	23.7 ± 0.1 185 ± 1	4.4 ± 0.2 335 ± 11	100.0 ± 0.0 146 ± 2	24.2 ± 0.1 186 ± 18	4.5 ± 0.1 324 ± 1
1	100.0 ± 0.0 89 ± 1	47.2 ± 0.2 229 ± 14	9.6 ± 0.2 321 ± 13	100.0 ± 0.0 85 ± 4	48.1 ± 0.1 225 ± 13	9.6 ± 0.2 301 ± 24
2	100.0 ± 0.0 61 ± 9	93.1 ± 0.9 308 ± 7	20.0 ± 0.2 365 ± 8	100.0 ± 0.0 59 ± 5	96.9 ± 0.3 331 ± 19	20.1 ± 0.2 359 ± 12
Bile is recycled						
0.5	128 ± 1	675 ± 64	3636 ± 125	131 ± 7	684 ± 25	3704 ± 44
1	84 ± 6	439 ± 29	2386 ± 96	89 ± 3	444 ± 33	2334 ± 71
2	62 ± 1	297 ± 1	1546 ± 95	66 ± 7	287 ± 40	1552 ± 90

Table 2: Bioaccessibility (%) and half life (CTS) for the fatty acids as a function of the IDF/(FA+MG) mass ratio. The result is expressed as the average and standard deviation of triplicates. When bile is recycled, the bioaccessibility is necessarily 100 % so only half life is reported.

IDF/(FA+MG) mass ratio	TC+vitA	TO+vitA	TEP-DH+vitA	TC+vitE	TO+vitE	TEP-DH+vitE
Bile is saturated						
0.5	9.2 ± 1.2 450 ± 21	2.6 ± 0.2 246 ± 33	3.6 ± 1.0 268 ± 86	97.2 ± 2.5 313 ± 34	26.2 ± 10.6 274 ± 77	26.0 ± 2.6 216 ± 48
1	12.6 ± 2.2 264 ± 42	8.0 ± 1.5 285 ± 71	4.3 ± 1.8 314 ± 128	97.0 ± 2.6 146 ± 15	64.3 ± 6.1 300 ± 48	24.8 ± 0.3 226 ± 73
2	11.8 ± 0.7 149 ± 23	24.5 ± 5.7 597 ± 43	8.5 ± 1.3 482 ± 80	98.7 ± 2.3 97 ± 12	97.3 ± 0.6 150 ± 16	40.7 ± 10.3 263 ± 66
Bile is recycled						
0.5	9.5 ± 1.4 306 ± 10	35.2 ± 4.4 1312 ± 150	86.2 ± 1.9 6238 ± 853	98.0 ± 1.7 209 ± 24	100.0 ± 0.0 752 ± 48	100.0 ± 0.0 2367 ± 488
1	11.0 ± 1.1 213 ± 19	38.8 ± 3.8 837 ± 94	91.6 ± 2.7 3739 ± 568	97.8 ± 2.6 161 ± 51	100.0 ± 0.0 557 ± 79	100.0 ± 0.0 1572 ± 149
2	14.2 ± 1.4 146 ± 14	43.9 ± 3.2 556 ± 37	95.2 ± 3.1 2147 ± 300	97.7 ± 1.9 102 ± 16	100.0 ± 0.0 285 ± 21	100.0 ± 0.0 1212 ± 206

Table 3: Same as table 2 for vitamins.

Length	TC+vitA	TO+vitA	TEP-DH+vitA	TC+vitE	TO+vitE	TEP-DH+vitE
Bile is saturated						
50	100.0 ± 0.0 122 ± 10	48.0 ± 0.2 324 ± 8	8.8 ± 0.4 687 ± 30	100.0 ± 0.0 130 ± 14	48.2 ± 0.2 353 ± 2	8.4 ± 0.4 647 ± 21
75	100.0 ± 0.0 96 ± 4	47.8 ± 0.3 253 ± 3	9.3 ± 0.2 417 ± 17	100.0 ± 0.0 98 ± 2	47.9 ± 0.2 272 ± 9	9.3 ± 0.1 426 ± 27
100	100.0 ± 0.0 89 ± 1	47.2 ± 0.2 229 ± 14	9.6 ± 0.2 321 ± 13	100.0 ± 0.0 85 ± 4	48.1 ± 0.1 225 ± 13	9.6 ± 0.2 301 ± 24
Bile is recycled						
50	111 ± 6	592 ± 15	3116 ± 55	114 ± 8	598 ± 41	3100 ± 64
75	93 ± 3	476 ± 24	2600 ± 47	93 ± 6	474 ± 11	2650 ± 19
100	84 ± 6	439 ± 29	2386 ± 96	89 ± 3	444 ± 33	2334 ± 71

Table 4: Bioaccessibility (%) and half life (CTS) for the fatty acids as a function of droplet length.

Length	TC+vitA	TO+vitA	TEP-DH+vitA	TC+vitE	TO+vitE	TEP-DH+vitE
Bile is saturated						
50	6.6 ± 1.8 347 ± 50	3.9 ± 0.2 362 ± 170	2.5 ± 0.8 244 ± 73	100.0 ± 0.0 267 ± 62	68.7 ± 1.2 309 ± 166	47.3 ± 2.3 356 ± 128
75	9.5 ± 1.8 221 ± 24	4.3 ± 1.2 347 ± 150	3.3 ± 0.4 398 ± 20	99.1 ± 1.6 195 ± 33	60.9 ± 10.3 199 ± 19	22.7 ± 5.1 369 ± 135
100	12.6 ± 2.2 264 ± 42	8.0 ± 1.5 285 ± 71	4.3 ± 1.8 314 ± 128	97.0 ± 2.6 146 ± 15	64.3 ± 6.1 300 ± 48	24.8 ± 0.3 226 ± 73
Bile is recycled						
50	9.6 ± 1.7 316 ± 41	20.3 ± 5.5 1080 ± 96	65.1 ± 8.4 5234 ± 359	98.0 ± 2.0 183 ± 14	100.0 ± 0.0 614 ± 165	100.0 ± 0.0 1855 ± 195
75	8.9 ± 0.7 222 ± 24	33.0 ± 4.0 1006 ± 56	90.1 ± 0.5 3807 ± 339	96.7 ± 3.7 142 ± 48	100.0 ± 0.0 461 ± 122	100.0 ± 0.0 1468 ± 28
100	11.0 ± 1.1 213 ± 19	38.8 ± 3.8 837 ± 94	91.6 ± 2.7 3739 ± 568	97.8 ± 2.6 161 ± 51	100.0 ± 0.0 557 ± 79	100.0 ± 0.0 1572 ± 149

Table 5: Same as table 4 for vitamins.

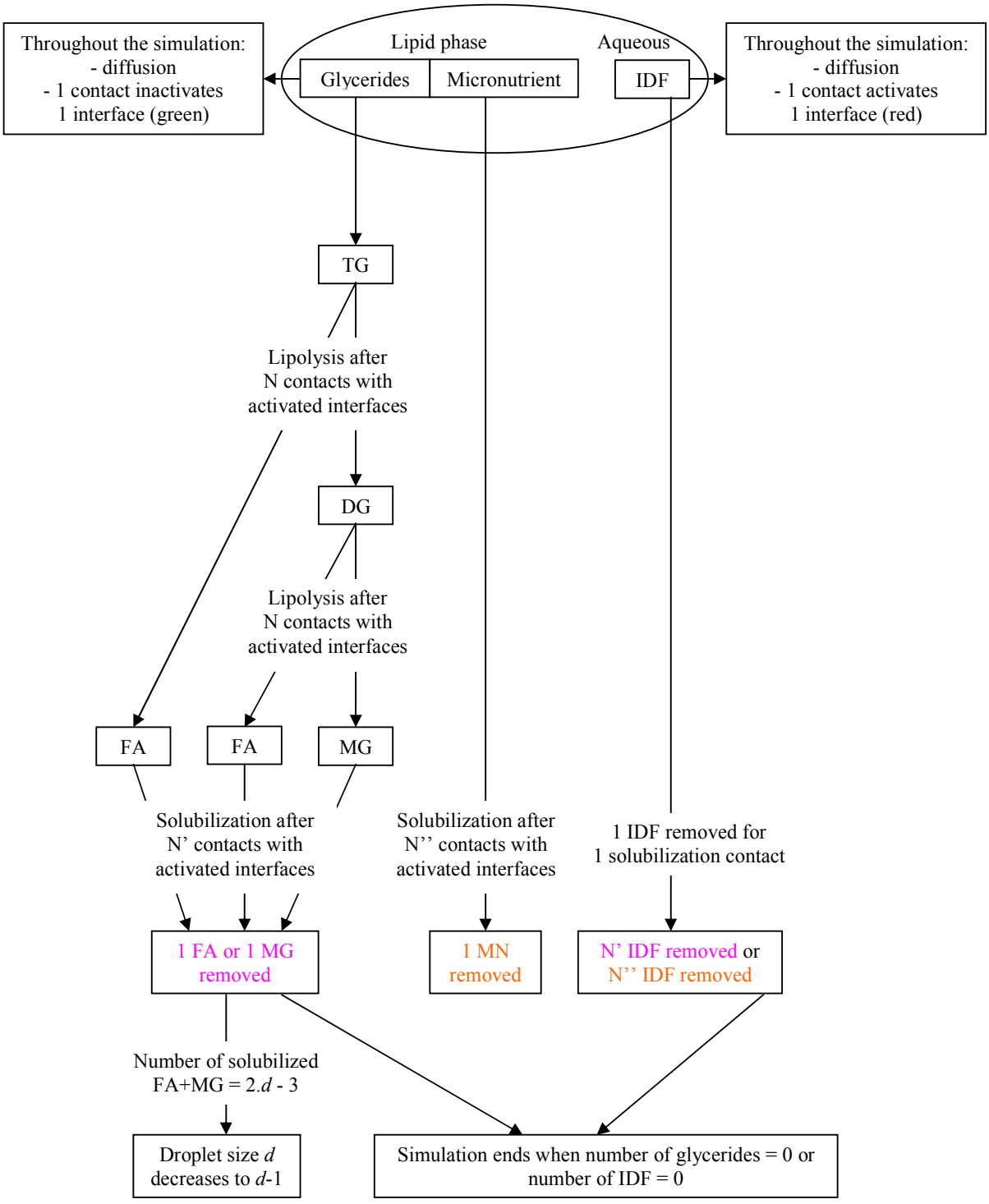

Figure 1: Diagram summarizing the simulation rules in the case where bile is saturated. In the case where bile is recycled, the same diagram applies except no IDF are removed. The numbers N, N' and N'' are taken inversely proportional to LR, SR and SR respectively.

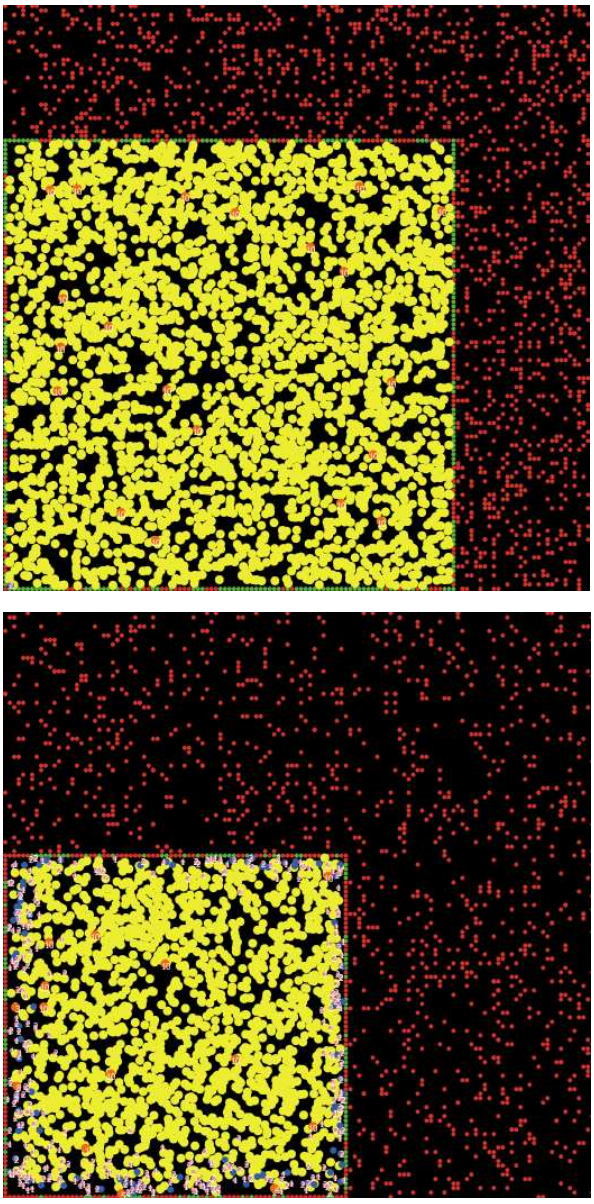

Figure 2: Pictures from a simulation of the digestion of TO+vitE with a droplet length of 100 and a IDF/(FA+MG) mass ratio of 2 (bile is saturated). Top: first step of the simulation, bottom: step at which half of the bile was saturated. TG is yellow, MN is orange, IDF is red, interface is green, DG is blue, MG and FA are pink. The numbers represent the number of contacts needed to solubilize the products in bile.

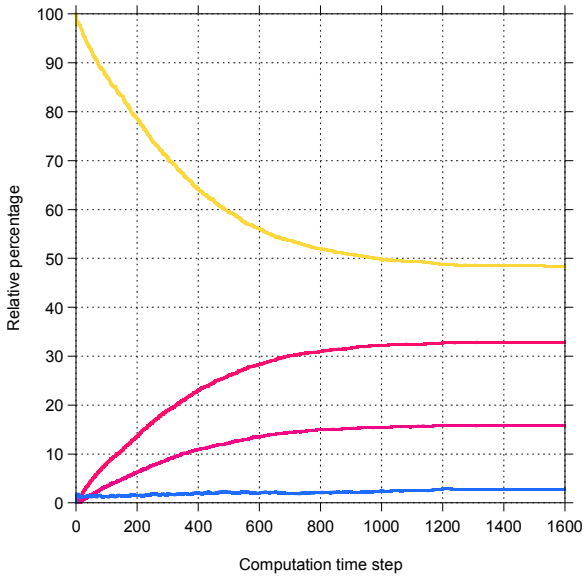

Figure 3: Representative result for the relative percentage of glycerides from a simulation of the digestion of TO+vitA with a droplet length of 100 and a IDF/(FA+MG) mass ratio of 1 (bile is saturated). Same colors as figure 2.

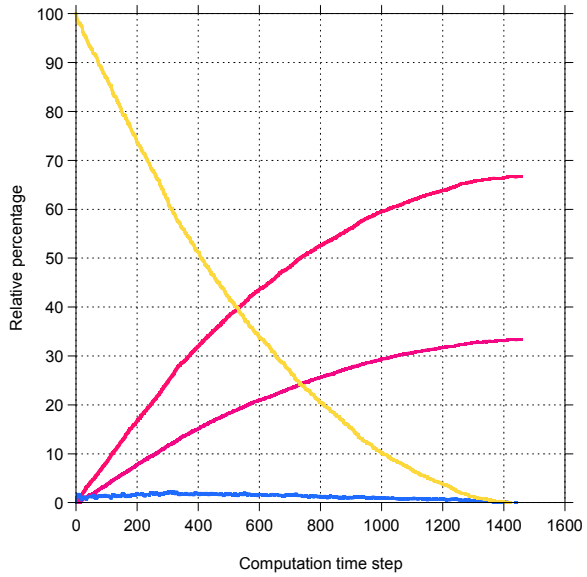

Figure 4: Same as figure 3 except bile is recycled.

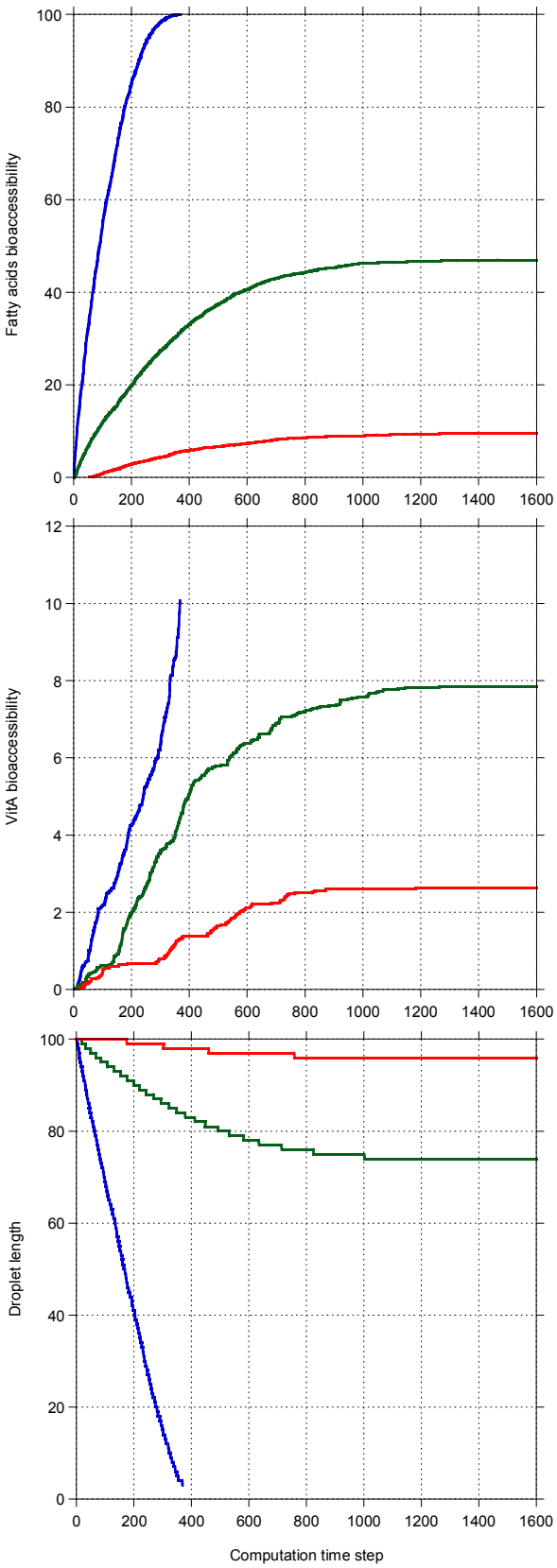

Figure 5: A representative set of results from a simulation of the digestion of various TG+vitA with a droplet length of 100 and a IDF/(FA+MG) mass ratio of 1 (bile is saturated). TC is blue, TO is green and TEP-DH is red.

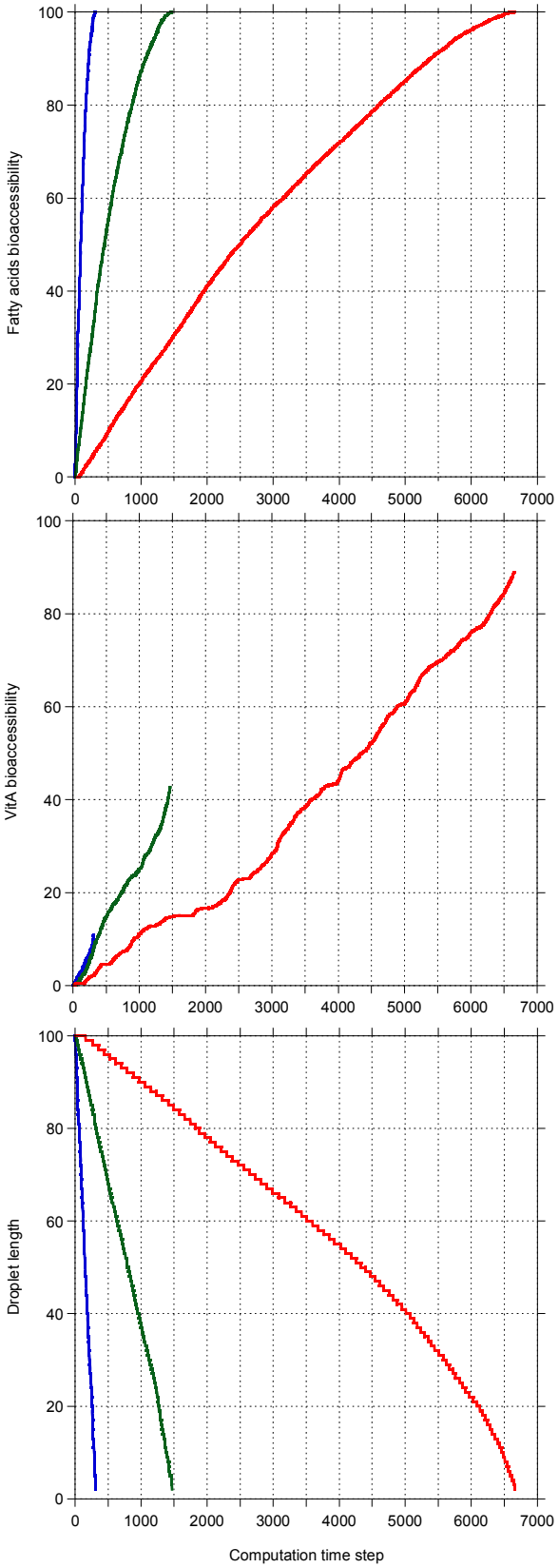

Figure 6: Same as figure 5 except bile is recycled.

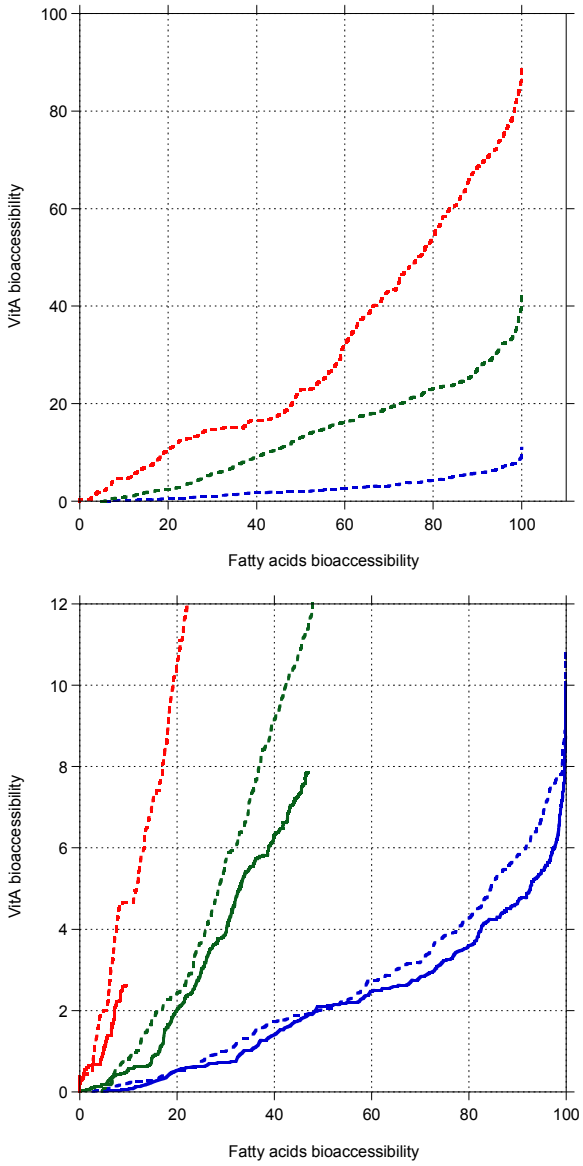

Figure 7: VitA bioaccessibility as a function of fatty acids bioaccessibility. Top: data from figure 6. Bottom: close-up to compare data from figure 6 (dashed lines, bile is recycled) and data from figure 5 (full lines, bile is saturated).

Graphical abstract: Study of the parameters influencing the intestinal digestion and bioaccessibility of lipophilic nutrients and micronutrients using a coarse-grained simulation.